Proceedings World Geothermal Congress 2020+1
Reykjavik, Iceland, April - October 2021

Effect of Silica Scaling Inhibitor in Geothermal Brine

Jan Přikryl and Kristján F. Alexandersson

Gerosion Ltd., Árleynir 2-8, IS-112 Reykjavík, Iceland

jan@gerosion.com

Keywords: geothermal, scaling, silica, inhibitor

ABSTRACT

Silica scaling is among the major limiting factors in increased energy extraction from geothermal fluids in the geothermal industry. Commonly, reinjection of brine is conducted at high temperature to overcome potential silica scale formation which can occur due to cooling. Silica and silicates have prograde solubility (i.e. decreasing solubility with decreasing temperature) and are anticipated to scale for example in heat exchangers at temperatures below 80-150°C depending on aqueous silica concentration. The aim of this study was to explore the optimal conditions to minimise or avoid scaling from the geothermal brine upon cooling. A series of laboratory experiments with and without commercial silica inhibitors were conducted as a function of temperature and pH, and silica concentration/scaling was monitored in the solution over time. The rates of initial silica scaling due to aqueous silica polymerisation may be delayed in order to reduce silica scaling using such inhibitors in geothermal equipment. Recent achievements have demonstrated that silica scaling can be controlled during geothermal fluid production at lower temperatures, thereby increasing energy output from geothermal power plants. This work was conducted in the GeoSmart project. The overall aims of the project are: 1) reduced geothermal energy cost, 2) reduced carbon footprint, 3) competitiveness in smart and flexible operation.

1. INTRODUCTION

Silica scaling is among the major limiting factors in increased energy extraction from geothermal fluids. Commonly, reinjection of brine is conducted at high temperature to overcome potential silica scale formation with cooling. Recent achievements in Iceland have demonstrated that silica scaling can be controlled during geothermal fluid production at lower temperatures (40-80°C), thereby increasing energy output from geothermal power plants.

Geothermal fluids contain many chemical components, which originate from the source fluid, magma gases and from dissolving host rocks within the reservoirs at high temperature. For many utilised geothermal systems, fluids are flashed to generate steam to power low pressure turbines. The flashed steam concentrates the dissolved components (gases in the steam phase and solutes in the liquid phase) and decrease fluid temperature and pressure. As a result, solids (minerals) may become supersaturated to form scales on the surfaces of piping, vessels, pumps, and other associated equipment (e.g. Gallup and von Hirtz 2010). Carbonates with sulphates have retrograde solubility, increased at low temperature, and are not expected to deposit, for instance upon cooling but are instead common scales associated with boiling and phase separation in boreholes, pipes and separators. Silica and silicates have prograde solubility (i.e. decreasing solubility with decreasing temperature) and are anticipated to scale for example in heat exchangers at temperatures below 80-150°C depending on aqueous silica concentration. Fairly common precipitates that deposit from geothermal brines include metal silicates, clays, calcium carbonates, sulphates, sulphides, arsenides and antimonides, and calcium fluoride. In hypersaline brines, flashing of steam can lead to halite precipitation. Dissolved silica is the most common precipitate to form upon flashing steam and/or cooling of geothermal brine (Gallup and Hirtz 2015).

Many high-temperature geothermal systems are characterised by fluids with elevated carbon dioxide (CO_2) and hydrogen sulphide (H_2S) concentrations. Such high temperatures together with the aggressive nature of the fluids can result in leaching of the reservoir rocks. This results in increased solute concentration of the geothermal fluids and eventually saturation with many geothermal minerals including silica (Figure 1). Here shown as a reaction controlled by quartz solubility (Fournier and Rowe 1966, Mahon 1966):

$$SiO_{2(s)} + H_2O \rightarrow H_4SiO_{4\,(aq)} \tag{1}$$

If metal ions are also present, silicates with Al, Fe, Mg and/or Ca and silica can form. Quartz and crystalline silica polymorphs have slow precipitation kinetics and their deposition is negligible. On the other hand, amorphous silica and/or silicates precipitate rapidly, in a matter of seconds to hours depending on conditions, in the fluid (Benning and Waychunas 2008) or via polymerisation of aqueous silica followed by aggregation, cementation and deposition. This process may either occur within solution leading to “floating” silica polymers, or on surfaces forming scales (Figure 2). Among factors controlling the rate of silica polymerisation are solution pH, ionic strength, temperature and level of supersaturation. The two pathways (polymerisation and aggregation in solution and on surfaces), plus settling of polymeric silica from solution, determine if polymerisation treatment to reduce silica deposition from spent geothermal waters will work.

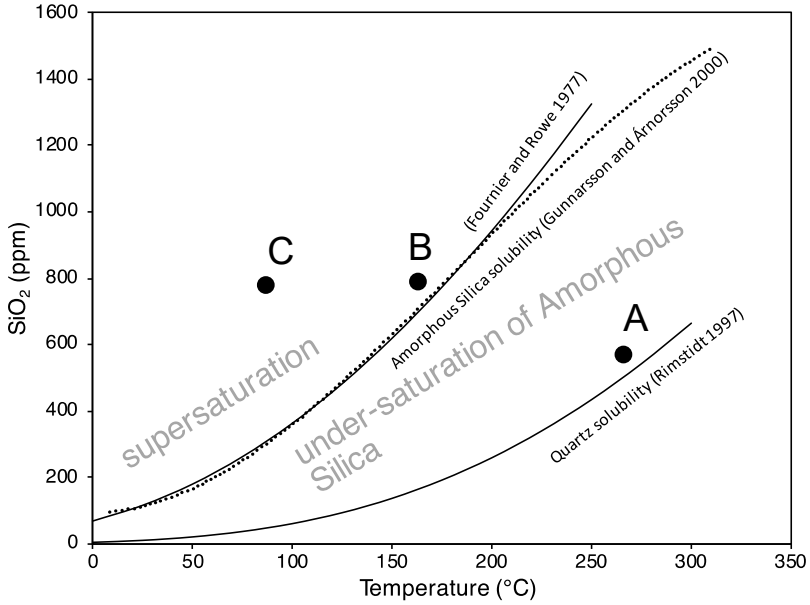

Figure 1: Temperature dependence of solubility of quartz and amorphous silica. The quartz, SiO_2, or alternatively chalcedony and silicates are dissolved and results in the formation of silicic acid. This is presented as point A. Point B is where the concentration of silicic acid reaches saturation with respect to amorphous silica, typically during flashing and cooling. Point C represents further cooling of the flashed brine.

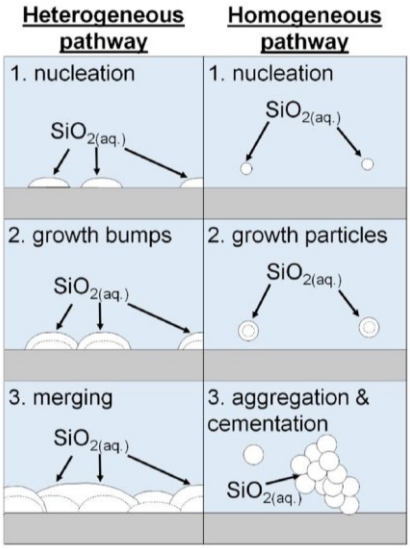

Figure 2: Schematic of the two silica precipitation pathways ($SiO_{2(aq)}$) = silica monomers in solution) inside the pipelines of geothermal power plant illustrated by van den Heuvel et al. 2018. Heterogeneous pathway is deposition onto surfaces (scaling) and homogeneous pathway is the polymerisation process.

Several methods have been utilised to decrease silica scaling in geothermal installations. The selected method is usually based on specific brine chemistry and process conditions and is not universally applicable. Some methods are even combined and deployed in boreholes, piping and equipment. Among methods to inhibit, remove or control scale deposits are:

- Controlled precipitation with metals (Rothbaum 1976).
- Forced precipitation of silica by cationic surfactants (Veda et al. 2000).
- Use of evaporation/percolation ponds (Mercado 1975).
- Practice of aging in retention pond (Yanagase et al. 1970).
- Crystallisation/clarification (Featherstone and Powell 1981).
- Dilution of silica concentration of brine with steam condensate or freshwater (Gallup and Featherstone 1985).

- Organic inhibitors/dispersants (Candelaria et al. 1996, Harrar et al. 1982, Gallup and Barcelon 2005).
- Injection of hot brine to avoid silica supersaturation or injection at near amorphous silica saturation (Henley 1983).
- Chelating agents, organic acids and complexing agents (Gallup 1997).
- Adjustment of pH (Rothbaum et al. 1979, Hibara et al. 1990).
- Maintenance of brine flash pressure and temperature to avoid silica supersaturation (von Hirtz 2016).

The rate of silica scaling has been widely studied and is dependent on factors such as the fluid temperature, pH, salinity/ionic strength, and concentration of certain cations in the case of silicates (e.g. Carroll et al. 1998, Dixit et al. 2016, Henley 1983, Mroczek et al. 2017, Sigfússon and Gunnarsson 2011). Scale can deposit instantaneously or be kinetically hindered for a significant amount of time. Experience shows that the best method to prevent silica and silicates scaling is based on a combination of preliminary models, laboratory and field testing for individual geothermal installation. Theoretical, and to some extent laboratory, scaling predictions have limitations. Firstly, physiochemical conditions within geothermal power plant may undergo short- and long-term changes: e.g. temperature, short travel distances and fast flow rates. This is cumbersome to simulate with thermodynamic models or a simple laboratory setup. Secondly, if the thermodynamic model is updated with kinetic precipitation it will not achieve accurate scaling prediction anyways because the kinetics of silica polymerisation and silica particle formation are still not fully described (review by Tobler et al. 2017).

The work described here focused on reducing silica scaling by application of scale inhibitors and pH modification. A series of laboratory experiments with and without commercial silica inhibitors was conducted as a function of temperature and pH, and silica concentration/scaling was monitored in the solution over time. Experimentally obtained scaling rates are applied to the scaling equation model developed in GeoSmart project to provide practical estimation of scaling over prolonged time to overcome limited theoretical forecasts.

2. MATERIALS

Three merchants supplied silica scale inhibitors/dispersants: Producer I, Producer II and Producer III. The producers and products are anonymized. As expected for commercial products, inhibitor formulations are trademark secrets of the vendors. However, Material Safety Data Sheets (MSDS) are available and indicate several possible components present in these inhibitors as phosphonic acids, phosphonates, acrylate polymers, polyacrylamides, oxyethylenes, sulfonates, carboxylic acid, and similar compounds. The dosage used in experiments is the dosage recommended by each vendor. In cases when the effluent brine shows excessive flocculation, the inhibitor concentration is advised to be reduced. Table 1 provides a list of the tested inhibitors.

Producer	**Product**	**#**
Producer I	I	1
Producer II	II	2
Producer III	III	3

Table 1: Inhibitors used for reducing silica scaling in geothermal environment.

3. METHODS

The simulated environment in the laboratory is based on field conditions at an undisclosed geothermal power plant. Experimental conditions have similar SiO_2 (~500 mg/kg) and Cl (~250-350 mg/kg) concentration to the discharged water from field scenario.

The stock solutions of silica were made by dissolving silica gel (Merck) into 0.1 M NaOH at room temperature. The next day the solution was filtered through a 0.2 µm filter and stored at room temperature. The solution was stable for months with SiO_2 concentration ≥5000 ppm. In order to start the experimental run the stock solution was diluted with deionised water to reach the desired SiO_2 concentration and pH was adjusted with hydrochloric acid (0.1 M HCl) to fit the required starting value. The pH decrease caused saturation with respect to amorphous silica. The experiments were carried out in 0.5 L polypropylene (PP) bottles and stirred with magnetic stir bars, placed in a temperature controlled water bath (Figure 3). The temperature range was 40-70±0.5°C and pH ~6.5-9.5 range for performed experiments.

Samples were collected periodically with decreasing frequency as solutions were approaching the silica equilibrium solubility concentration. A small aliquot of 2.5 ml was collected and cooled down in few seconds for pH measurements at room temperature. Another 0.5 ml of experimental solution was extracted and diluted with deionised water, 9.5 ml, previously acidified with 0.04 ml of concentrated HCl (1:1). Acid was added to prevent silica deposition during sample storage. Monomeric aqueous silica concentrations were analysed using the molybdosilicate method (Fishman and Friedman 1989). Samples (0.5 ml) at the beginning and at the end of experiments were collected too, diluted with deionised water (9.5 ml) and acidified with nitric acid for ICP-OES analyses to confirm amount of dissolved silica. The analytical precision based on repeated analysis of an internal standard at the 95% confidence level was 3.7% for Si. The percent error of the screening tests was determined to be about 5%.

Baseline silica precipitation experiments and the model of silica scaling potential formulated in GeoSmart project are utilised in this report and compared with the performance of scale inhibitors. Rate of monomeric SiO_2(aq) decrease to form SiO_2(aq) polymers may be described by the rate function,

$$\frac{dm_{SiO_{2(aq)}}}{dt} = -k\left(m_{SiO_{2(aq)}} - m_{SiO_{2(aq),eq}}\right)^4 \quad (2)$$

where k is the overall rate constant of monomeric transformation to silica tetramers, $m_{SiO_{2(aq)}}$ is the concentration of monomeric SiO_2(aq) in solution and $m_{SiO_{2(aq),eq}}$ is the equilibrium concentration of SiO_2(aq) with respect to amorphous silica.

Geochemical modelling was conducted with aid of PHREEQC software version 3 (Parkhurst and Appelo 2013) and phreeqc.dat database, suitable for simulations of geothermal settings at low temperatures (Horbrand et al. 2018). Secondary scaling and its precipitated volume per liter of brine is presented and can be easily upscaled and used to determine clogging hazards.

Figure 3: Setup used for silica scaling experiments.

4. RESULTS AND DISCUSSION

Table 2-5 presents the results of the laboratory tests, baseline experiments without any inhibitors (Table 2) and each set of inhibitors (Tables 3-5). The recommended dosage of inhibitor by each vendor was applied in all experimental inhibitor runs. No run showed excessive flocculation and therefore dosage adjustments were not necessary. In all instance the experiments were allowed to reach close to equilibrium/solubility concentration to evaluate variations in formation rate. The concentration is monitored as a function of time, and temperature and pH. Loss in SiO_2 concentration is presented as a „polymerised“ amount of the initial concentration and graphically presented on Figures 4-7. The baseline experiments, (Table 2, Figure 4) show both the experimental values and calculated values based on the precipitation model.

The kinetic delay in polymerisation is obvious in the baseline experiments. It is approximately 15 minutes before the change in SiO_2 concentration is observed in all tested conditions, more precisely 10 minutes at neutral pH at 40°C. This kinetic formation delay can be prolonged with the aid of inhibitors, and was found in all tested conditions. All the inhibitors show the best inhibiting performance approximately during the first hour. Later on, the formation rate of polymerised silica is somewhat close to or at baseline rate for tested conditions until reaching solubility concentration.

In general, inhibitors managed to reduce the rate of forming amorphous silica most effectively at close to neutral pH at 40°C. When temperature is kept at 40°C and pH is alkaline, ~9.5, the difference to the baseline SiO_2 precipitation rate is not large, (Tables 2-5), because the rate of amorphous silica polymerisation is already relatively low for these conditions. Higher temperature helps to lower the scaling formation speed because of higher silica solubility at higher temperature. When temperature is raised to 70°C and pH is lowered to ~8 the inhibition rate is comparable to the rate at pH ~9.5/40°C. However, the SiO_2 concentrations are close to the baseline concentrations after ca. 30 minutes and best results were obtained with II inhibitor. The advantage of the higher temperature is the solubility for amorphous silica is higher and therefore less scaling can form. Higher pH values decreased the rate of polymerisation. Inhibitors managed to decrease the polymerisation rate at neutral pH and 40°C to the rates occurring at alkaline pH or higher temperature for about 100 minutes in case of I and II inhibitor solutions, and for a little bit shorter duration with III inhibitor.

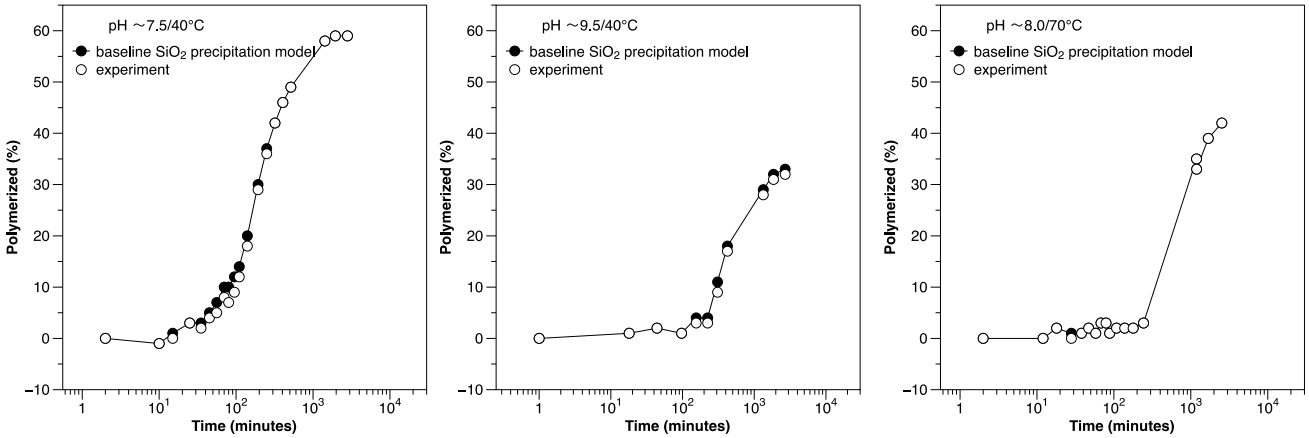

Figure 4: Experimental vs model of amorphous silica formation in baseline settings.

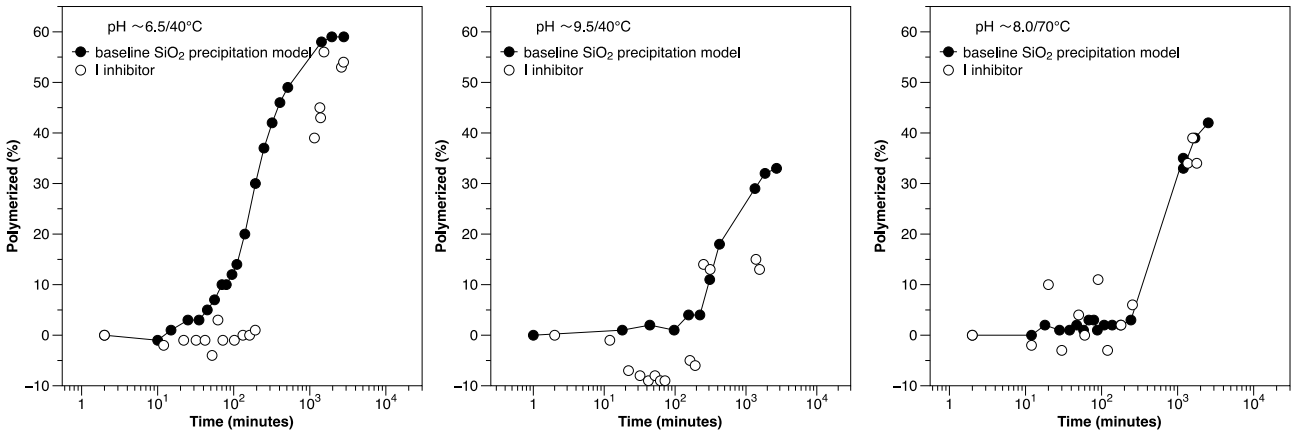

Figure 5: Silica polymerisation in the solution, precipitation model vs I inhibitor.

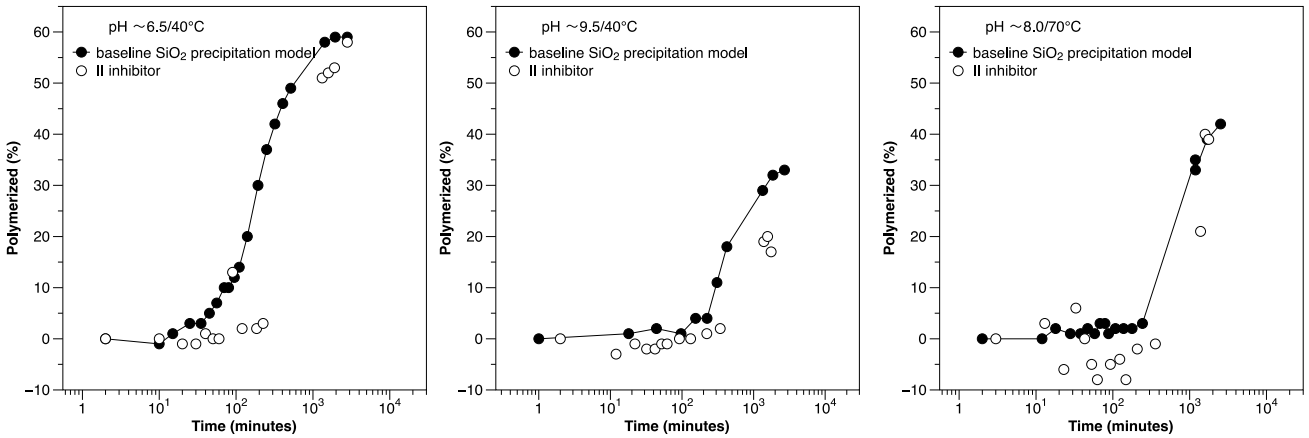

Figure 6: Silica polymerisation in the solution, precipitation model vs II inhibitor.

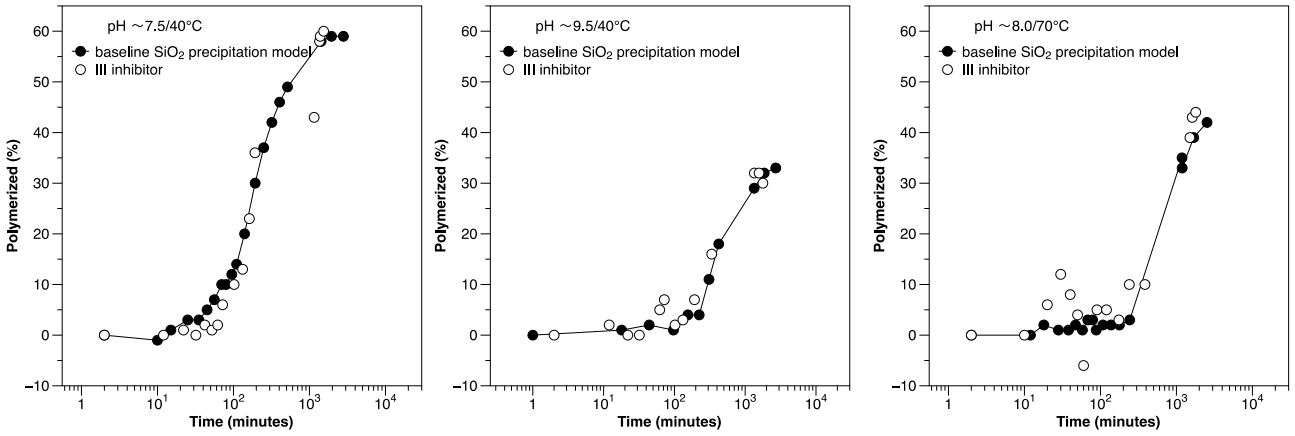

Figure 7: Silica polymerisation in the solution, precipitation model vs III inhibitor.

Experiment	Temp.	Sample	Time	pH_{23}°C	SiO_2 (exp.)	SiO_2 (calc.)	Polymerized	
no inhibitor	°C	#	minutes		ppm	ppm	(exp.) %	(calc.) %
blank 1	40	1	2	7.72	472	473	0	0
blank 1	40	2	10		478	465	-1	-1
blank 1	40	3	15		471	461	0	1
blank 1	40	4	25		460	453	3	3
blank 1	40	5	35		464	445	2	3
blank 1	40	6	45		455	438	4	5
blank 1	40	7	56	7.68	448	431	5	7
blank 1	40	8	70		435	422	8	10
blank 1	40	9	80		437	416	7	10
blank 1	40	10	95		428	408	9	12
blank 1	40	11	110		414	401	12	14
blank 1	40	12	140		385	387	18	20
blank 1	40	13	193		335	367	29	30
blank 1	40	14	250		301	349	36	37
blank 1	40	15	320	7.53	275	332	42	42
blank 1	40	16	405		256	314	46	46
blank 1	40	17	515	7.50	240	296	49	49
blank 1	40	18	1425	7.36	199	223	58	58
blank 1	40	19	1950		194	203	59	59
blank 1	40	20	2800	7.60	193	182	59	59
blank 2	40	1	1	9.54	479	481	0	0
blank2	40	2	18		475	478	1	1
blank2	40	3	44		470	474	2	2
blank 2	40	4	97		476	467	1	1
blank 2	40	5	155		466	460	3	4
blank 2	40	6	224	9.60	464	451	3	4
blank 2	40	7	308		434	442	9	11
blank 2	40	8	423	9.64	397	430	17	18
blank 2	40	9	1338	9.74	347	367	28	29
blank 2	40	10	1858		330	344	31	32
blank 2	40	11	2700	9.76	327	316	32	33
blank 3	70	1	2	8.02	494	494	0	0
blank 3	70	2	12		494	492	0	0
blank 3	70	3	18		482	491	2	2
blank 3	70	4	28		491	489	0	1
blank 3	70	5	38		487	488	1	1
blank 3	70	6	47		483	486	2	2
blank 3	70	7	58		487	485	1	1
blank 3	70	8	68		481	483	3	3
blank 3	70	9	79		481	481	3	3
blank 3	70	10	88	8.03	490	480	1	1
blank 3	70	11	108		482	477	2	2
blank 3	70	12	138		483	473	2	2
blank 3	70	13	178		485	468	2	2
blank 3	70	14	243		478	459	3	3
blank 3	70	15	1185	8.17	319	380	35	35
blank 3	70	16	1190		329	380	33	33
blank 3	70	17	1688		301	355	39	39
blank 3	70	18	2528	8.23	288	324	42	42

Table 2: Summary of the baseline silica formation, no inhibitor, tests.

Experiment I Inhibitor	Temp. °C	Sample #	Time minutes	$pH_{23}°C$	SiO_2 (exp.) ppm	Polymerized (exp.) %
I A	40	1	2	6.25	512	0
I A	40	2	12	6.22	522	-2
I A	40	3	22		518	-1
I A	40	4	32		515	-1
I A	40	5	42		517	-1
I A	40	6	52		534	-4
I A	40	7	62		496	3
I A	40	8	72		517	-1
I A	40	9	102		515	-1
I A	40	10	132		514	0
I A	40	11	162		514	0
I A	40	12	192		509	1
I A	40	13	1152	6.45	311	39
I A	40	14	1357		281	45
I A	40	15	1387		289	43
I A	40	16	1537		227	56
I A	40	17	2607		238	53
I A	40	18	2779		234	54
I B	40	1	2	9.57	493	0
I B	40	2	12		496	-1
I B	40	3	22		527	-7
I B	40	4	32		530	-8
I B	40	5	42		536	-9
I B	40	6	52		534	-8
I B	40	7	62		535	-9
I B	40	8	72		535	-9
I B	40	9	162		517	-5
I B	40	10	192		523	-6
I B	40	11	252		424	14
I B	40	12	312		431	13
I B	40	13	1382	9.68	417	15
I B	40	14	1554		431	13
I 70	70	1	2	7.68	486	0
I 70	70	2	12		497	-2
I 70	70	3	20		437	10
I 70	70	4	30		501	-3
I 70	70	5	50		466	4
I 70	70	6	60		487	0
I 70	70	7	90		431	11
I 70	70	8	120		500	-3
I 70	70	9	180		477	2
I 70	70	10	255		459	6
I 70	70	11	1358		323	34
I 70	70	12	1575		296	39
I 70	70	13	1785	7.9	319	34

Table 3: Results of I inhibitor performance.

ExperimeIIt	Temp.	Sample	Time	pH_{23}°C	SiO_2 (exp.)	Polymerized
II Inhibitor	°C	#	minutes		ppm	(exp.) %
II A	40	1	2	6.5	525	0
II A	40	2	10		526	0
II A	40	3	20		528	-1
II A	40	4	30		531	-1
II A	40	5	40		520	1
II A	40	6	50		524	0
II A	40	7	60		525	0
II A	40	8	90		454	13
II A	40	9	120		516	2
II A	40	10	185		516	2
II A	40	11	225		507	3
II A	40	12	1320		255	51
II A	40	13	1585		252	52
II A	40	14	1910		246	53
II A	40	15	2805	6.58	220	58
II B	40	1	2	9.58	539	0
II B	40	2	12		555	-3
II B	40	3	22		545	-1
II B	40	4	32		548	-2
II B	40	5	42		548	-2
II B	40	6	52		543	-1
II B	40	7	62		543	-1
II B	40	8	92		537	0
II B	40	9	132		537	0
II B	40	10	222		532	1
II B	40	11	342		528	2
II B	40	12	1387		436	19
II B	40	13	1567		433	20
II B	40	14	1757	9.72	447	17
II 70	70	1	3	7.73	480	0
II 70	70	2	13		465	3
II 70	70	3	23		509	-6
II 70	70	4	33		449	6
II 70	70	5	43		478	0
II 70	70	6	53		505	-5
II 70	70	7	63		519	-8
II 70	70	8	93		502	-5
II 70	70	9	123		499	-4
II 70	70	10	148		519	-8
II 70	70	11	208		488	-2
II 70	70	12	358		487	-1
II 70	70	13	1385		378	21
II 70	70	14	1588		287	40
II 70	70	15	1768	7.97	291	39

Table 4: Results of II inhibitor performance.

Experiment III Inhibitor	Temp. °C	Sample #	Time minutes	pH_{23}°C	SiO_2 (exp.) ppm	Polymerized (exp.) %
III A	40	1	2	6.92	546	0
III A	40	2	12		545	0
III A	40	3	22		540	1
III A	40	4	32		548	0
III A	40	5	42		533	2
III A	40	6	52		540	1
III A	40	7	62		533	2
III A	40	8	72		511	6
III A	40	9	102		489	10
III A	40	10	132		477	13
III A	40	11	162		420	23
III A	40	12	192		352	36
III A	40	13	1152		313	43
III A	40	14	1357		229	58
III A	40	15	1387		226	59
III A	40	16	1537	6.97	220	60
III B	40	1	2	9.52	523	0
III B	40	2	12		511	2
IIIB	40	3	22		523	0
III B	40	4	32		525	0
III B	40	5	62		495	5
IIIB	40	6	72		488	7
III B	40	7	102		514	2
III B	40	8	132		509	3
IIIB	40	9	192		487	7
III B	40	10	337		441	16
III B	40	11	1347		355	32
IIIB	40	12	1567		355	32
III B	40	13	1777	9.61	367	30
III 70	70	1	2	7.68	490	0
III 70	70	2	10		487	0
III 70	70	3	20		458	6
III 70	70	4	30		430	12
III 70	70	5	40		448	8
III 70	70	6	50		469	4
III 70	70	7	60		514	-6
III 70	70	8	90		462	5
III 70	70	9	120		460	5
III 70	70	10	175		470	3
III 70	70	11	240		439	10
III 70	70	12	385		436	10
III 70	70	13	1505		296	39
III 70	70	14	1615		277	43
III 70	70	15	1795	7.9	273	44

Table 5: Results of III inhibitor performance.

The inhibitor performance is transformed to volume of forming amorphous silica polymers per kilogram of solution to show potential scaling capacity (Figure 8). The initial polymerisation kinetic delay, even extended with inhibitors, is apparent in volume of forming scaling too. Equilibrium concentration are presented here as the volume of amorphous silica that can form in each solution as a function of time until reaching solubility limit. As expected, less silica can form at 70°C. The rate of polymerisation is very similar at pH 8/70°C and 9.5/40°C. When an inhibitor is used the rate can be slowed down to the same level as at neutral pH and 40°C, however the final volume/amount forming per kilogram of solution is different.

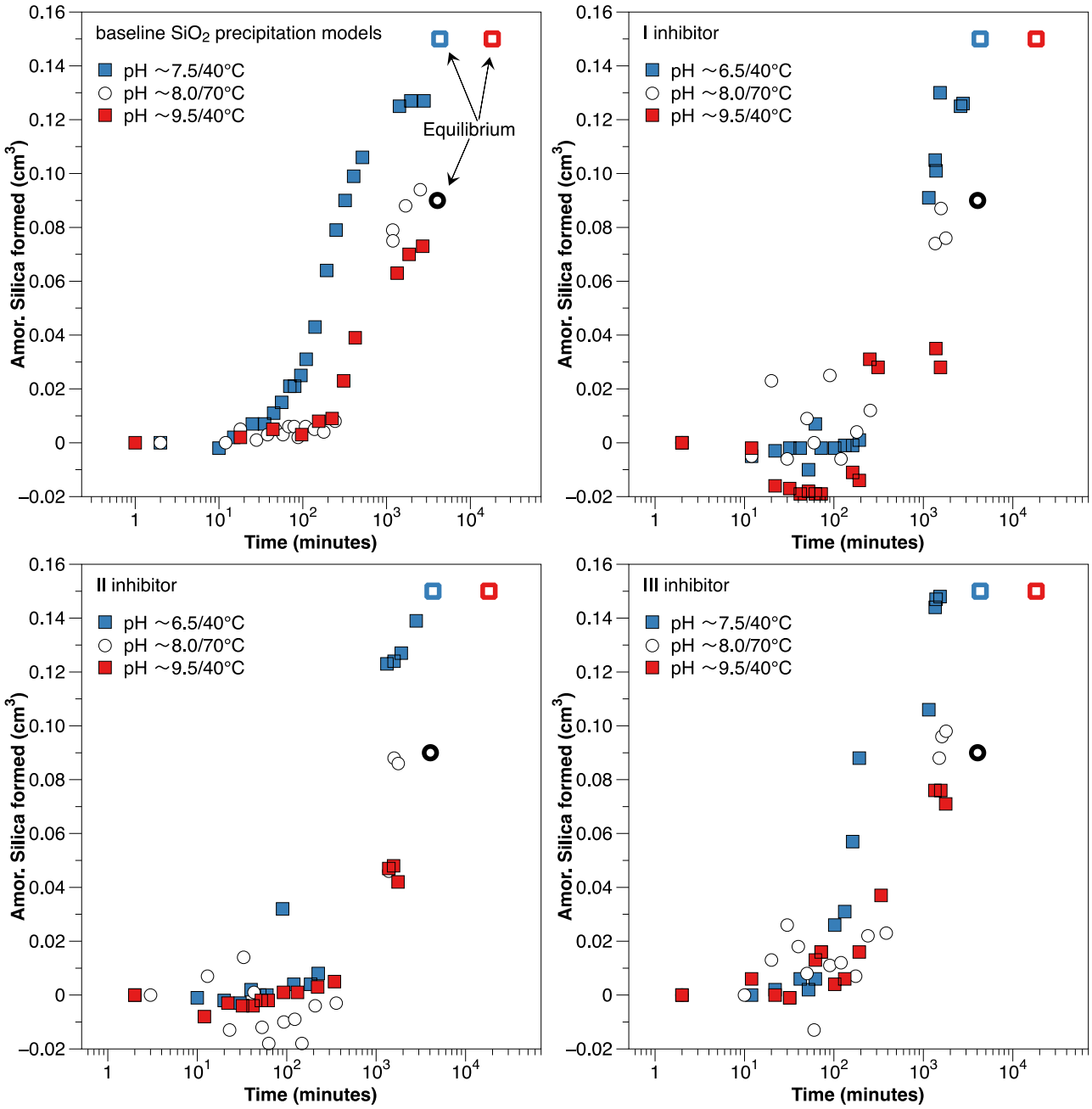

Figure 8: Summary of scaling potential as a function of time, temperature and pH for baseline solutions and for solutions with added inhibitors.

Field conditions are different than in the laboratory. The flow-rate was simulated by using stirring bars at approximately 60 rpm in the laboratory experiments. The flow regime and flow-rate co-controls the formation mechanism and rate in retention tanks of powerplant. Different amount of silica, different scale thickness, is developed for instance before and after heat exchanger and injection wells after the same amount of time (van den Heuvel et al. 2018). Therefore, field testing is desirable with operation parameter adjustments. The artificial solution is never the same as natural brine with respect to geochemistry, although it can serve as initial testing and optimization step.

5. CONCLUSIONS

The following conclusions are reported:

- Rate of experimental silica polymerisation is similar at neutral pH at 70°C to alkaline pH at 40°C. The fastest polymerisation and shortest induction period with biggest scaling potential had neutral pH at 40°C. Scaling potential is lowest at 70°C due to higher solubility. However, scaling can be precipitated with control by pH adjustment in retention tank for field conditions, assuming rapid supersaturation and fast polymerisation rate.

- In general silica scaling can be decreased with aid of commercial inhibitors that were tested here, most effectively in neutral pH at 40°C. Inhibitors were able to prolong the kinetic delay from around 15 minutes up to 100 minutes until the polymerisation and

precipitation occurs with the typical silica polymerisation rate for given conditions. Inhibitor II and I performed better than III inhibitor in tested conditions.

ACKNOWLEDGEMENTS

This work is part of the H2020 EU project GeoSmart (no. 818576) funded from the European Union's Horizon 2020 research and innovation program.

REFERENCES

Benning, L. G., and Waychunas, G. A.: Nucleation, growth, and aggregation of mineral phases: Mechanisms and kinetic controls. In Kinetics of Water-Rock Interaction, Springer, New York, NY. (2008), 259-333.

Candelaria, M. N. R., Garcia, S. E., Baltazar Jr, A. D. J., and Solis, R. P.: Methods of coping with silica deposition-the PNOC experience (No. CONF-960913-), Geothermal Resources Council, Davis, CA (United States), (1996).

Carroll, S., Mroczek, E., Alai, M., and Ebert, M.: Amorphous silica precipitation (60 to 120 °C): Comparison of laboratory and field rates. *Geochimica et Cosmochimica Acta*, **62(8)**, (1998), 1379-1396.

Dixit, C., Bernard, M. L., Sanjuan, B., André, L., and Gaspard, S.: Experimental study on the kinetics of silica polymerization during cooling of the Bouillante geothermal fluid (Guadeloupe, French West Indies), *Chemical Geology*, **442**, (2016), 97-112.

Featherstone, J. L., and Powell, D. R.: Stabilization of highly saline geothermal brines, *Journal of Petroleum Technology*, **33(04)**, (1981), 727-734.

Fishman, M. J., and Friedman, L. C.: Techniques of water-resources investigations of the United States Geological Survey, Methods for determination of inorganic substances in water and fluvial sediments, (1989).

Fournier, R. O., and Rowe, J. J.: Estimation of underground temperatures from the silica content of water from hot springs and wet-steam wells, *American Journal of Science*, **264(9)**, (1966), 685-697.

Gallup, D. L.: U.S. Patent No. 5,665,242, Washington, DC: U.S. Patent and Trademark Office, (1997).

Gallup, D. L., and Barcelon, E.: Investigations of organic inhibitors for silica scale control from geothermal brines–II. *Geothermics*, **34(6)**, (2005), 756-771.

Gallup, D. L., and Featherstone, J. L.: U.S. Patent No. 4,522,728, Washington, DC: U.S. Patent and Trademark Office, (1985).

Gallup, D. L., and von Hirtz, P. N.: Control of silica scaling in geothermal systems using silica inhibitors, chemical treatment, and process engineering, In The Science and Technology of Industrial Water Treatment, CRC Press, (2010), 160-182.

Gallup, D. L., and von Hirtz, P. N.: Control of silica-based scales in cooling and geothermal systems, In Mineral Scales and Deposits, Elsevier, (2015), 573-582.

Harrar, J. E., Locke, F. E., Otto Jr, C. H., Lorensen, L. E., Monaco, S. B., and Frey, W. P.: Field tests of organic additives for scale control at the Salton Sea geothermal field, *Society of Petroleum Engineers Journal*, **22(01)**, (1982), 17-27.

Henley, R. W.: pH and silica scaling control in geothermal field development, *Geothermics*, **12(4)**, (1983),307-321.

Hibara, Y., Tazaki, S., and Kuragasaki, M: Advanced H_2S gas treatment system for geothermal power plant–"geothermal gas injection technology.", *Geotherm. Sci. & Tech*, **2**, (1990), 161-171.

Hörbrand, T., Baumann, T., and Moog, H. C.: Validation of hydrogeochemical databases for problems in deep geothermal energy. *Geothermal Energy*, ***6(1),*** (2018).

Mahon, W. A. J.: Silica in hot water discharged from drillholes at Wairakei, New Zealand, *New Zealand Jour. Sci*, **9**, (1966), 135-144.

Mercado, S.: Cerro Prieto geothermal electric project: pollution and basic protection, in: 2nd UN Geothermal Symposium, (1975), 1394-1398.

Mroczek, E., Graham, D., Siega, C., and Bacon, L.: Silica scaling in cooled silica saturated geothermal water: Comparison between Wairakei and Ohaaki geothermal fields, New Zealand, *Geothermics*, **69**, (2017), 145-152.

Parkhurst, D. L., and Appelo, C. A. J.: Description of input and examples for PHREEQC version 3: a computer program for speciation, batch-reaction, one-dimensional transport, and inverse geochemical calculations (No. 6-A43), US Geological Survey, (2013).

Rothbaum, H. P.: Removal of Silica and Arsenic from Geothermal Discharge Waters by Precipitation of Useful Calcium Silicates, In Proc. Second UN Symp. Devel. Use Geother. Res., Vol. 2, (1976), 1417-1425.

Rothbaum, H. P., Anderton, B. H., Harrison, R. F., Rohde, A. G., and Slatter, A.: Effect of silica polymerisation and pH on geothermal scaling. *Geothermics*, **8(1)**, 1979, 1-20.

Sigfusson, B., and Gunnarsson, I.: Scaling prevention experiments in the Hellisheiði power plant, Iceland. In Proceedings, thirty-sixth workshop on geothermal reservoir engineering, Stanford University, Stanford, California, SGP-TR-191, (2011).

Tobler, D. J., Stawski, T. M., and Benning, L. G.: Silica and alumina nanophases: natural processes and industrial applications, In New Perspectives on Mineral Nucleation and Growth, Springer, (2017), 293-316.

van den Heuvel, D. B., Gunnlaugsson, E., Gunnarsson, I., Stawski, T. M., Peacock, C. L., and Benning, L. G.: Understanding amorphous silica scaling under well-constrained conditions inside geothermal pipelines, Geothermics, **76**, (2018), 231-241.

Veda, A., Kato, K., Abe, K., Furokawa, T., Mogi, K., and Ishimi, K.: Recovery of silica from the Sumikawa geothermal fluids by addition of cationic reagents. *Journal of the Geothermal Research Society of Japan*, **22(4)**, (2000), 249-258.

von Hirtz, P.: Silica scale control in geothermal plants—historical perspective and current technology, In Geothermal Power Generation, Woodhead Publishing, (2016), 443-476.

Yanagase, T., Suginohara, Y., and Yanagase, K.: The properties of scales and methods to prevent them. *Geothermics*, **2**, (1970), 1619-1623.